Asian Journal of Chemistry; Vol. 37, No. 2 (2025), 266-274

ASIAN JOURNAL OF CHEMISTRY

https://doi.org/10.14233/ajchem.2025.32957

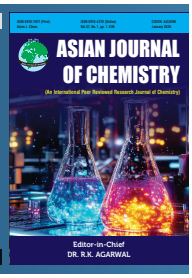

In vitro Antibacterial, Antifungal, Cytotoxicity and Molecular Docking Studies of Transition Metal(II) Complexes Derived from New Quinoline Schiff Base

BALIRAM TUKARAM VIBHUTE*, and AMOL JAGANNATH GHOTI*

Department of Chemistry, Doshi Vakil Arts and G.C.U.B. Science & Commerce College, Goregaon-402103, India

*Corresponding authors: E-mail: vbtchem@gmail.com; ghotiamol@gmail.com

Received: 27 October 2024; *Accepted*: 12 December 2024; *Published online*: 31 January 2025; AJC-21875

The synthesis of new quinoline based Schiff base and its metal complexes *viz*. Co^{2+}, Cu^{2+}, Ni^{2+} & Cd^{2+}, were synthesized and characterized. The Schiff base was prepared by condensation of 2-hydroxy-7-methoxyquinoline-3-carbaldehyde and *p*-methylbenzene sulfonohydrazide. The structure of Schiff base and its metal(II) complexes were characterized through different physical and analytical techniques *i.e.*, FTIR, ^{1}H NMR, ^{13}C NMR, ESR, ESI-MS, electronic spectra, elemental analysis and TGA. Magnetic susceptibility values indicate that Cu(II), Co(II) and Ni(II) complexes were paramagnetic in nature. Low molar conductivity values reveal that all the metal complexes are non-electrolytic in nature. Furthermore, all the compounds were subjected to *in vitro* biological activity and computational docking studies. The results showed that the Schiff based ligand and its metal(II) complexes exhibited higher activity against the A-549 cancer cell line and lower in case of the MCF-7 cancer cell lines compared to standard drug paclitaxel. Furthermore, the molecular docking study shows the significant binding affinity of metal complexes with tubulin protein. Hence, all the synthesized Schiff base metal complexes have excellent biological activity and could be act as potential anticancer agents.

Keywords: Quinoline, Schiff base, Metal(II) complexes, Biological activity, Molecular docking, Cytotoxicity.

INTRODUCTION

The Schiff bases containing ONO donor atoms showed significant biological activity and it helps to easily bind with transition and non-transition metal ions [1-3]. The binding of organic moiety with copper, cobalt and nickel showed good results in the biological activities [4]. The presence of the azomethine functional group in the metal complex was found to be important for biological activity. Various azomethines were known to have important anticancer [5], antifungal [6], antibacterial [7] and diuretic activities [8].

Schiff bases featuring heterocyclic moieties have been a prominent research field with extensive literature available on Schiff base complexes incorporating heterocyclic structures [9]. Among the heterocyclic compounds, the metal complexes derived from quinoline compounds are currently attracting more attention than the Schiff bases derived from other chemical classes; this is because of wide applications of quinoline in biological and pharmaceutical activities such as cytotoxicity [10], antimicrobial [11], antitubercular [12], antioxidant [13], DNA binding study [14], *etc*.

In view of important features of Schiff base containing quinoline moiety [15], in this work, a new quinoline Schiff base ligand, (*E*)-N′;-((2-hydroxy-7-methoxyquinolin-3-yl)methylene)-4-methylbenzenesulfonohydrazide, was synthesized from (*E*)-*N*′-((2-hydroxy-6-methyl-quinolin-3-yl)methylene)-4-methylbenzenesulfonohydrazide and (*E*)-*N*′-((2-hydroxyquinolin-3-yl)methylene)-4-methyl-benzenesulfonohydrazide. The Schiff base ligand were further used to synthesize metal(II) complexes with Cu^{2+}, Ni^{2+}, Co^{2+} and Cd^{2+} and screened for the mycobacterial, DNA binding and cytotoxicity studies.

EXPERIMENTAL

The analytical grade metal(II) salts, solvents and primary aromatic amines were purchased from Molychem, Mumbai (India) and Sigma-Aldrich Chemicals (USA) and used as such without further purification. ^{1}H and ^{13}C NMR spectra of ligand were recorded in DMSO-d_6 solvent on Bruker Avance 400 MHz and 100 MHz spectrometers, respectively and tetramethylsilane (TMS) was used as internal standard. Electronic spectra were recorded using Carry 100 UV-visible spectrophotometer. FTIR

This is an open access journal, and articles are distributed under the terms of the Attribution 4.0 International (CC BY 4.0) License. This license lets others distribute, remix, tweak, and build upon your work, even commercially, as long as they credit the author for the original creation. You must give appropriate credit, provide a link to the license, and indicate if changes were made.

spectra were recorded on a Nicolet iS10, thermos Scientific, USA spectrophotometer using KBr pellets in 4000–400 cm^{-1} range. The magnetic moment of the prepared complexes were measured by the Gouy method at 25 ºC using the MKl Johnson Matthey model. Molar conductance was measured on a DDS-11C type conductivity bridge in DMSO at th concentration of 10^{-3} M. Thermogravimetric analysis (TGA) was performed on Mettler-Toledo instrument at the heating range 20 ºC/min with a temperature range of 25 to 1000 ºC. High resonance Mass spectra were recorded on a Waters Micromass Q-Tof Micro with electrospray ionization (ESI) and atmospheric pressure chemical ionization (APCI) sources. ESR spectrum of Cu(II) complex was performed on JES-FA200 ESR spectrometer. CHNS analyses were performed on a FLASH EA 1112 series instrument.

Synthesis of ligand: 2-Chloro-7-methoxyquinoline-3-carbaldehyde was synthesized from starting material 3-methoxy aniline by acylation followed by Vilsmeier-Haack reaction as per reported method [16]. The obtained compound was further used for the synthesis of 2-hydroxy-7-methoxyquinoline-3-carbaldehyde by refluxing 2-chloro-7-methoxyquinoline-3-carbaldehyde (10 mmol) and H_2O (1 mL) in acetic acid (5 mL) for 4 h after that the reaction mass was transferred into ice-cold water. The obtained product was filtered, washed with distilled water and purified in hot ethanol to obtain a corresponding pure product, 2-hydroxy-7-methoxyquinoline-3-carbaldehyde, as an intermediate. The obtained intermediate was further used for the formation of the corresponding ligand.

Then, a mixture of obtained intermediate compound (1 mmol), *p*-methylbenzenesulfonohydrazide (1 mmol) and acetic acid (5-10 drops) in ethanol (10 mL) was refluxed at 80 ºC for 4 h. The progress of the reaction was checked by TLC. The reaction mixture was transferred into crushed ice and extracted with ethyl acetate (2 × 15 mL). The organic extracts were washed with brine solution (2 × 15 mL) and dried over anhydrous sodium sulfate. The solvent was evaporated under reduced pressure to afford the corresponding crude compound. The obtained crude compound was recrystallized using ethanol. Yield: 78%, m.p.: 222-224 ºC (**Scheme-I**). Elemental analysis of $C_{18}H_{17}N_3O_4S$ (m.w.: 371.41), calcd. (found) %: C, 58.18 (58.21); H, 4.45 (4.61); 11.36 (11.31); S, 8.78 (8.63). ^{1}H NMR (DMSO-d_6, δ ppm): 11.69 (s, 1H, NH), 11.34 (s, 1H, OH), 8.10 (s, 1H, Ar-H), 8.08 (s, 1H, Ar-H), 7.25-7.23 (d, H, Ar–H, J = 7.5 Hz), 7.70 (s, 1H, Ar–C=CH), 7.18-7.15 (d, 1H, Ar–H, J = 8 Hz), 6.98-6.96 (d, 1H, Ar–H, J = 8 Hz), 3.73 (s, 3H, -OCH_3) and 2.30 (s, 3H, –CH_3); ^{13}C NMR: (100 MHz, DMSO-d_6, δ ppm): 161.06, 154.87, 143.54, 142.21, 136.51, 134.67, 133.91, 129.67, 127.46, 125.31, 121.02, 119.83, 116.96, 109.26, 55.65 and 21.52.

Synthesis of metal(II) complexes: The synthesis of metal (II) complexes was performed by adding 25 mL hot ethanolic metal(II) chloride solution (2.5 mmol) to 25 mL hot ethanolic Schiff base solution (5 mmol) in 2:1 (ligand:metal) proportion. The reaction mixture was stirred for 30 min and then a few drops of 5% NaOH solution were added to maintain the basic pH of the reaction medium followed by refluxation for 4 h. The obtained coloured precipitate was filtered, washed with distilled water followed by ethanol and finally dried in an oven for 90 min at 80 ºC (**Scheme-II**).

Biological study

Antibacterial study: The minimum inhibitory concentration (MIC) of ligand and its metal(II) complexes was carried out by the broth dilution method [17-22]. DMSO used as a diluent and served as a negative control [23]. Two Gram-positive bacteria *viz. Staphylococcus aureus* (MTCC 96) and *Streptococcus pyogenes* (MTCC 442) and two Gram-negative bacteria *viz. Escherichia coli* (MTCC 443) and *Pseudomonas aeuruginosa* (MTCC 1688) were tested against the synthesized compounds with ampicillin and chloramphenicol as the standard reference drugs [18]. Serial dilutions of ligand and its metal(II) complexes were prepared in primary and secondary screening. The control plate with no prepared compounds and drugs was subculture spreading evenly over a plate suitable for the growth of selected bacterial pathogens and kept overnight at 37 ºC in incubator. The MIC of the control bacterial strain was assessed to check the efficacy of the reference drug concentrations. The lowest concentration was recorded as the MIC. The amount of growth from the control plate before incubation was compared. Synthesized compounds were diluted to 2000 µg/mL concentration as a stock solution. In primary screening, 125, 250 and 500 µg/mL concentrations of synthesized compounds were taken. The synthesized compounds found active in primary screening were further tested in the second set of dilutions against all

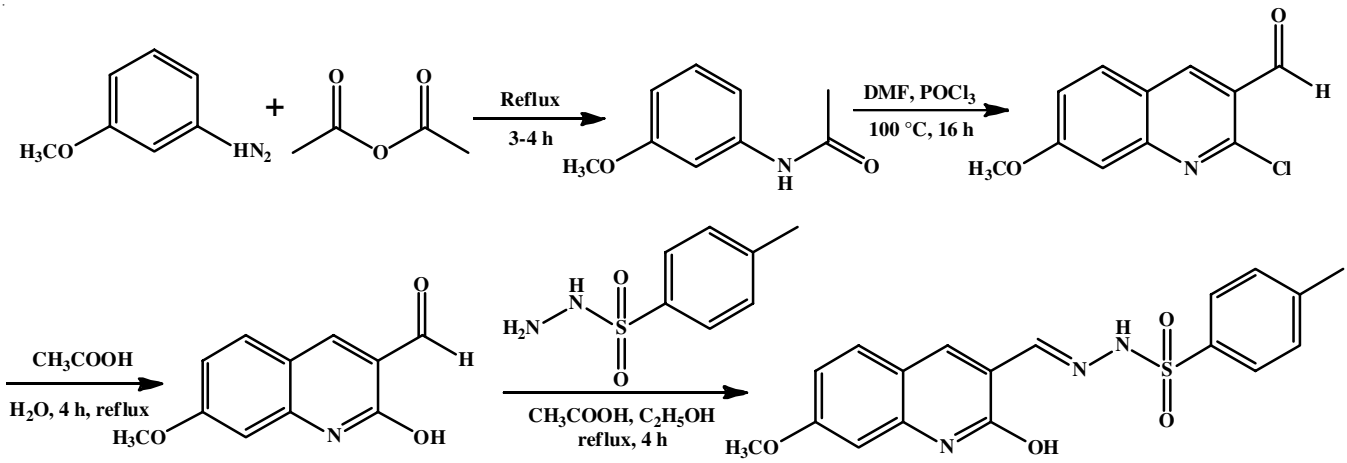

Scheme-I: Synthesis of ligand, (E)-N′-((2-hydroxy-7-methoxyquinolin-3-yl) methylene)-4-methylbenzenesulfonohydrazide

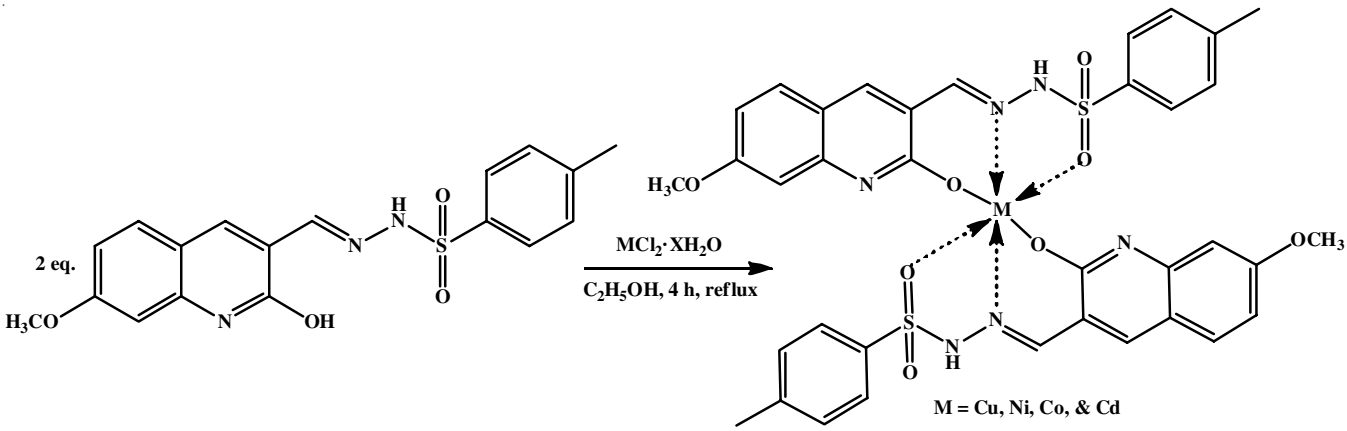

Scheme-II: Synthesis of metal complexes

the selected pathogens. The compounds found active in primary screening were diluted similarly to 100, 50, 25, 12.5, 6.250, 3.125 and 1.5625 µg/mL concentrations. The MIC was considered for the dilution showing at least 99% inhibition.

Antifungal studies: Antifungal activity of synthesized compounds was examined with three fungal strains *viz.*, *Candida albicans* (MTCC 227), *Aspergillus niger* (MTCC 282) and *A. clavatus* (MTCC 1323) using the agar dilution method [18]. To determine MIC, a stock solution of the synthesized compounds was prepared in DMSO and then incorporated in a specified quantity of sterile molten dextrose agar. Inoculums were prepared by diluting stock to 100 mL of nutrient broth in 250 mL sterilized and clean conical flasks. The conical flasks were incubated at 27 ºC for 24 h prior to the experiment. The plates were kept under aseptic conditions to allow the diffusion of the solution properly into the potato-dextrose agar medium. Then, the plates were incubated at 25 ºC for 48 h. The highest dilution displaying at least 99% inhibition zone was taken as MIC against griseofulvin and nystatinas standards. The triplicate analysis was performed to minimize errors.

Cytotoxicity studies: The synthesized ligand and its metal(II) complexes were evaluated for their cytotoxicity against the A-549 (human lung cancer) and MCF-7 (human breast cancer) cell lines by using MTT [3-(4,5-dimethylthiazol-2-yl)-2,5-diphenyltetrazolium bromide] assay. These cells were seeded at a density of approximately 5×10^3 cells well in a 96-well flat bottom microtitre plate and maintained at 37 ºC overnight in 95% humidity and 5% CO_2. Different concentrations (50, 40, 30, 20, 10, 5 µM) of samples were treated and the cells were incubated for next 48 h. Then cells in the wells were washed twice with phosphate buffer saline (PBS) and 20 µL of MTT [3-(4,5-dimethythiazol-2-yl)-2,5-diphenyltetrazolium bromide] staining solution (5 mg mL^{-1} in phosphate buffer saline) was added to each well and the plate was incubated at 37 ºC. After 4 h, 100 µL DMSO was added to each well to dissolve the formant crystals. Absorbance was recorded at 570 nm using a microplate reader. Paclitaxel was used as a standard drug during the activity check. Each reading was performed in three types for each concentration. Results are expressed as mean ± standard deviation (n = 3). The percentage cell viability of the cells was calculated using the following relation:

$$\text{Viability (\%)} = \frac{\text{Mean OD of test compound}}{\text{Mean OD of negative control}} \times 100$$

Inhibiting cells (%) = 100 – Surviving cells

The IC_{50} was extrapolated from the dose-response curve. The synthesized compound concentration that reduced the viability of cells by 50% (IC_{50}) was calculated by plotting triplicate data points over a concentration range and calculating the values using GraphPad Prism Ver.5.1-program.

Molecular docking studies: Molecular docking was employed to investigate the binding mode of metal complexes with the tubulin receptor protein using AutoDock4 software [24]. The microtubules are essential in cell division, mitosis and intracellular transport [25]. The microtubules are cytoskeleton filamentous and are formed through the polymerization of α- and β-tubulin heterodimers [26]. Disruption of microtubule dynamics can induce cell cycle arrest in the G2-M phase of the cell cycle and leads to cell apoptosis [27]. Hence, microtubules become an important and attractive drug target for anticancer drug design. It has been shown that naturally occurring compounds such as paclitaxel, vinblastine and colchicine exert their effect by affecting α- and β-tubulin structure and dynamics [26,28,29]. In this study, we used paclitaxel as a control for the biological study along with the metal(II) complexes. The paclitaxel binds to the taxol site of β-tubulin and stabilizes the microtubule dynamics [30]. Hence, we used β-tubulin protein as the target receptor for the docking study to understand the binding mode of various metal complexes. The crystal structure of tubulin bound with paclitaxel was taken from the protein database (source code: 1JFF.pdb). The crystal structure of 1JFF.pdb is crystallized from bovine at the resolution of 3.50 Å [31]. The atomic coordinates of the metal complexes (Co, Cd, Cu and Ni) were built and optimized using Avogadro [32]. Here, the paclitaxel binding site of β-tubulin is considered for molecular docking study. For docking, a grid box of 80 × 80 × 80 grid points and a grid spacing of 0.375 Å were built around the paclitaxel binding site of β-tubulin. Here, we keep tubulin protein rigid and metal complexes as flexible, similar to an earlier study [33]. The output conformations were generated by applying the Lamarckian Genetic Algorithm. These output conformations were further clustered using an all-atom RMSD

with a cut-off of 4 Å. The clusters were further analyzed based on binding energy, van der Waals, inter-molecular energies, *etc*. The least energy-docked conformation of metal complexes was further used for the analysis of bonding and non-bonding interactions using PyMol [34] and Discovery Studio visualiser, respectively.

RESULTS AND DISCUSSION

The synthesized Schiff base containing quinoline moeity as ligand and their metal(II) complexes were subjected to elemental analysis. The elemental experimental values for the ligand and its metal(II) complexes were matched with the theoretical values (Table-1). The conductance values of complexes were in the range of 36-57 Ω^{-1} cm^2 mol^{-1}, representing the non-electrolytic character of the complexes [35]. Moreover, it also proves that the coordination spheres of the metal complexes do not contain any water molecules [36].

FT-IR spectra: To determine the characteristic vibration bands between the ligand and their metal complexes, all the synthesized compounds were subjected to FT-IR spectral analysis. The peak observed in the Schiff base ligand at 1660 cm^{-1} due to the azomethine ν(C=N) stretching was shifted to a lower wavenumber (1632-1620 cm^{-1}) in the metal complexes indicating the participation of azomethine nitrogen in coordination with the metal ion (N-M) [37]. Similarly, the phenolic ν(O-M) stretching vibration band observed at 1352 cm^{-1} in free ligand is shifted to a lower frequency of 1082-1028 cm^{-1} region, also confirming the participation of the phenolic group in complex formation [38]. The vibration bands for the SO_2 group in the free ligand appeared at 1315 and 1184 cm^{-1} ($\nu_{asym}(SO_2)$) and ($\nu_{sym}(SO_2)$), respectively. In metal(II) complexes, the asymmetric and symmetric bands are shifted to 1235-1217 and 1123-1112 cm^{-1}, respectively, upon the coordination of the central metal ion [38-41]. The additional peaks observed in metal complexes in 465-458 cm^{-1} region were due to the N-M bonding and 512 to 506 cm^{-1} were due to O-M bonding [42-45]. The details of the key IR spectral bands are given in Table-2.

Electronic spectra and magnetic moment: All the synthesized metal(II) complexes were subjected to electronic spectra and magnetic moment. In electronic spectra, the transition bands for ligand was obtained at 322 and 370 nm; these transition is due to $\pi\rightarrow\pi^*$ and $n\rightarrow\pi^*$, respectively. For metal(II) complexes, these transition bands were shifted to higher wavelengths. For metal(II) complexes (Cu, Ni, Co and Cd), the transition bands are observed at 325 and 385, 349 and 396, 347 and 394, 357 and 394 nm, respectively. The shifting of the transition band at longer wavelengths in metal(II) complexes was due to the coordination of the Schiff base with the central metal ion [46].

The magnetic moment for Cu, Ni and Co was calculated by using the Gouy balance at 25 ºC. For Cu complex, the magnetic moment was observed as 1.80 B.M., which is close to spin only value for the octahedral geometry of copper(II) complexes [47]. The magnetic moment values for Ni(II) and Co(II) complexes were found to be 3.25 and 4.85 B.M, respectively, which is again equal to spin-only values for octahedral geometry for Ni(II) and Co(II) complexes [48,49].

ESR spectra: An ESR spectrum of Cu(II) complex was recorded in DMSO solvent at liquid nitrogen temperature (77 K) (Fig. 1). It gives information about the environment around the central metal ion in the complex. The spectrum shows a highly intense band in the higher magnetic field. The hyperfine interaction that occurred for the complex was due to the interface with oxygen and nitrogen nuclei nearby copper ions [50]. The Hamiltonian parameter was used to calculate the ground state of Cu(II) complex. Details of the calculated values are given in Table-3. The obtained g-values for the Cu complex are $g_{\parallel}$ 2.225 and $g_{\perp}$ 2.189. The obtained $g_{\parallel}$ and $g_{\perp}$ values are greater than g value for free electron 2.0023, which indicates that the complex is axially symmetrical with $d_{x^2-y^2}$ ground state, which is the characteristic of octahedral geometry [51].

TABLE-1
PHYSICAL AND ANALYTICAL DATA OF METAL(II) COMPLEXES OF QUINOLINE BASED SCHIFF BASE

Compounds (m.f.)	Yield (%)	m.p. (ºC)	λ_m (cm^2 Ω^{-1} mol^{-1})	μ_{eff} (B.M.)	m.w.	Elemental analysis (%): Found (calcd.)			
						C	N	H	S
Cu complex $(C_{18}H_{16}N_3O_4S)_2Cu$	72	280-282	36	1.80	803.35	53.66 (53.76)	10.23 (10.45)	3.87 (4.01)	7.76 (7.97)
Ni complex $(C_{18}H_{16}N_3O_4S)_2Ni$	83	> 300	38	3.25	799.50	54.07 (54.08)	10.44 (10.51)	3.90 (4.03)	8.20 (8.02)
Co complex $(C_{18}H_{16}N_3O_4S)_2Co$	68	> 300	47	4.85	799.74	54.15 (54.07)	10.39 (10.51)	4.13 (4.03)	8.02 (8.03)
Cd complex $(C_{18}H_{16}N_3O_4S)_2Cd$	81	> 300	57	Dimagnetic	854.22	50.43 (50.68)	9.71 (9.85)	3.66 (3.78)	7.51 (7.52)

TABLE-2
FT-IR STRETCHING FREQUENCY OF QUINOLINE BASED SCHIFF BASE AND ITS METAL COMPLEXES (cm^{-1})

Compounds	ν(C=N)	ν(C-O)	ν(N-M)	ν(O-M)	$\nu_{asym}(SO_2)$	$\nu_{sym}(SO_2)$
Ligand	1660	1352	–	–	1315	1184
Cu complex	1632	1053	465	508	1221	1112
Ni complex	1620	1084	465	512	1217	1113
Co complex	1620	1024	458	506	1235	1123
Cd complex	1629	1078	464	506	1221	1113

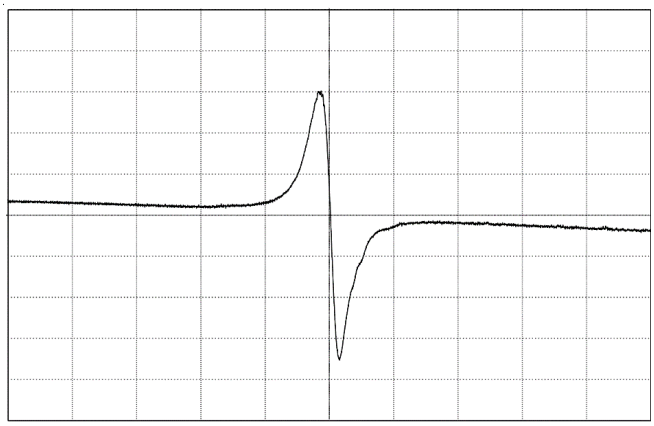

Fig. 1. ESR spectrum of Cu-complex

TABLE-3
ESR SPECTRAL DATA OF Cu COMPLEX

$G_{\perp}$	$g_{\parallel}$	$g_{avg.}$	G	$\mu_{eff.}$ (B.M.)
2.189	2.225	2.201	1.192	1.81

Mass spectra: The molecular ion peak of the Schiff base ligand showed at *m/z* 372.04, which was exactly matched with its calculated molecular weight. In metal(II) complexes, the highest mass peaks were obtained at *m/z* 802.77, 800.84, 800.80 and 855.39 for Cu^{2+}, Ni^{2+}, Co^{2+} and Cd^{2+} complexes, respectively. These obtained mass peaks are equal to their corresponding molecular weight. Hence, the obtained mass spectra support the proposed structure of the compounds.

Thermal studies: Thermal analysis was performed to gain significant information about the thermal stability of the synthesized metal complexes as well as whether the water molecules are inside or outside the inner coordination sphere of the metal [52-54]. Table-4 summarized with the decomposition stages, temperature range, loss of weight (actual and calculated) and assignments of the loss fragments. The thermogram of the Cu complex exhibited two decomposition stages. In stage first, the 35.36% weight loss (calculated 35.00%) was observed between the temperature range 180-460 ºC, which corresponds to the loss of toluene side chain of ligand moiety. In second stage, 40.48% weight loss was observed (calculated 39.50%) in the temperature range 480-960 ºC, which represents the loss of quinoline moiety of the coordinated ligand molecule. Finally, 13.07% residue remains present (calculated 13.25%), which was due to a metal with an organic moiety (Fig. 2).

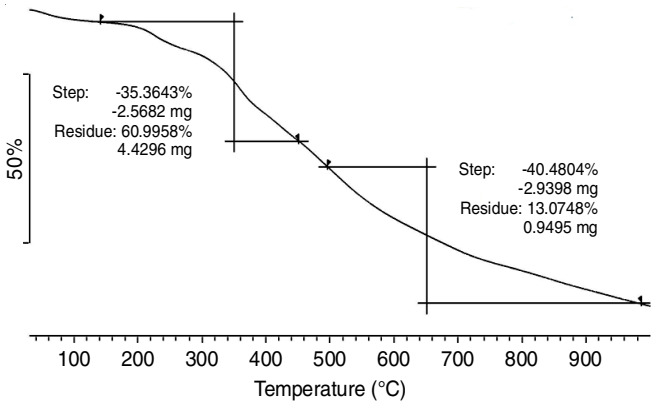

Fig. 2. Thermogram of Cu(II) complex

***In vitro* cytotoxicity:** *In vitro* cytotoxicity of Schiff base ligand and its metal(II) complexes was investigated against A-549 (human lung cancer) and MCF-7 (human breast cancer) cell lines and results are tabulated in Table-5. Paclitaxel was used as the standard drug during the activity check. The ligand and its metal(II) complexes showed inhibition of cell value IC_{50} in the range 43.10-58.47 µM for A-549 and 44.09-61.27 µM for MCF-7 cell lines. The ligand and its metal(II) complexes exhibited higher activity against the A-549 cancer cell line and lower in the case of the MCF-7 cancer cell line compared to standard. From the obtained results, it was observed that the synthesized metal(II) complexes were found to be more active than their corresponding ligand molecule. The order of activity of all the metal(II) complexes against A-549 cancer cell line is Ni > Cu > Co > Cd complex > Schiff base ligand.

Molecular docking studies: To explore the interaction of metal complexes (Cu^{2+}, Ni^{2+}, Co^{2+} and Cd^{2+}) with β-tubulin target receptor protein, we employed molecular docking using AutoDock4.2 software [23]. The least binding energy conformation of metal(II) complexes (Cd^{2+}, Co^{2+}, Cu^{2+} and Ni^{2+}) was found at -11.82, -11.53, -11.77 and -11.08 kcal/mol, respect-

TABLE-4
THERMAL DECOMPOSITION DATA OF METAL(II) COMPLEXES OF QUINOLINE BASED SCHIFF BASE

Complex formula	Decomposition temperature (°C)	Weight loss (%)		Assignment
		Observed	Calculated	
$(C_{18}H_{16}N_3O_4S)_2Cu$	180-480	35.36	35.00	$C_{14}H_{14}O_2S_2$
	480-960	40.48	39.50	$C_{20}H_{14}N_2O_2$
	Residue	13.07	13.25	$C_2H_4O_4Cu$
$(C_{18}H_{16}N_3O_4S)_2Ni$	180-320	32.53	32.91	$C_{11}H_9N_3O_3S$
	340-580	20.81	21.27	$C_{11}H_8NO$
	620-100	17.11	17.27	$C_7H_8N_2$
	Residue	21.47	22.65	$C_7H_7O_2Ni$
$(C_{18}H_{16}N_3O_4S)_2Co$	140-480	24.55	24.90	$C_{11}H_9N_3O$
	500-1000	33.68	32.91	$C_{11}H_9N_3O_3S$
	Residue	32.45	31.65	$C_7H_7O_4SCo$
$(C_{18}H_{16}N_3O_4S)_2Cd$	180-280	22.43	23.06	$C_8H_9N_3O_2S$
	300-660	29.70	28.92	$C_{11}H_9N_3O_4$
	Residue	31.23	31.01	C_9H_4OCd

TABLE-5
SHOWS THE *in vitro* CYTOTOXICITY DATA

Compound	IC_{50} values (μM)	
	A-549	MCF-7
Ligand	58.47	61.27
Cu-complex	45.45	56.49
Ni-complex	43.10	44.09
Co-complex	53.19	53.07
Cd-complex	54.34	46.77
Paclitaxel	69.54	30.76

ively (Table-6). All the metal(II) complexes show significant binding affinity with β-tubulin protein as shown in Fig. 3. All these metal complexes prefer the taxol site of β-tubulin [29]. Furthermore, analysis of the β-tubulin-Cd metal complex shows the conventional hydrogen bonding interaction of residue Thr276 (1.98 Å) and carbon-hydrogen bonding interaction of Thr276 (1.75 Å), His229 (2.30Å), Ala233 (2.76 Å) with Cd^{2+} metal complex (Fig. 4a). The His229 and Asp226 show the electrostatic interactions, Arg278 forms π-donor hydrogen bond, Thr276 makes π-lone pair bond and His229 makes π-π T-shaped interactions with Cd^{2+} complex (Fig. 4a). Moreover, hydrophobic π-alkyl type interactions are formed between β-tubulin residues, including Leu286, Leu217, Leu219, Arg278, Ala233, Pro274 and Leu231 and Cd metal complex.

TABLE-6
HYDROGEN BONDING INTERACTIONS (kcal/mol) OF β-TUBULIN RESIDUES WITH THE SYNTHESIZED METAL(II) COMPLEXES

Metal complexes	Binding energy	Atoms involved in the bonding interactions	Distance atom pair	Angle (°)
Cd complex	-11.82	Drug-H-O-THR276	1.98	121.49
		Drug-C-O-THR276	1.75	143.35
		Drug-C-O-ALA233	2.30	141.09
		Drug-N-H-HIS229	2.76	151.96
Co complex	-11.53	Drug-H-O-THR276	2.08	121.21
		Drug-CH-O-THR276	2.73	
Cu complex	-11.77	Drug-H-O-THR276	1.83	127.72
Ni complex	-11.08	Drug-H-O-THR276	1.78	151.73

The β-tubulin-Co^{2+} complex shows the residue Thr276 (121.21 Å) forms conventional as well as carbon-hydrogen bonding interaction with the Co^{2+} ion (Fig. 4b). The residue Asp226 forms electrostatic π-anion, Thr276 and Arg278 forms π-donor hydrogen bond, His229 forms hydrophobic π-π T-shaped interactions. In addition, Leu286 and Leu371 forms alkyl type of interactions with the Co^{2+} ion. Furthermore, the residues Leu231, Arg278, Leu219, Ala233, Pro274 and Leu371 make the hydrophobic π-alkyl type of interactions.

Simiarly, the β-tubulin-Cu and Ni complexes also show the residue Thr276 (127.72 Å & 1.78 Å) and makes the conventional hydrogen bonding interactions. The Ala233 forms carbon-hydrogen bonding interactions (Fig. 4c) with Cu^{2+} ions, while while the Pro360 (3.39) form with Ni^{2+} ions. In addition, His229 and Asp226 make electrostatic π-cation and π-anion interactions with Cu^{2+} ions, respectively, whereas Arg278 makes the π-donor hydrogen bonding. The residues Leu219, Thr276 and Leu286 form π-sigma, π-lone and alkyl type of interactions with the Cu^{2+} ions, whereas residues Leu217, Leu219, Arg278, Ala233, Pro274 and Leu371 make the hydrophobic π-alkyl type of interactions.

With Ni-metal complex, the Leu219 make the electrostatic π-sigma and hydrophobic π-alkyl type of interactions as shown in Fig. 4d. In addition, Asp226 forms π-anion, His229 forms π-π T-shaped and Arg-278 forms π-alkyl interactions with the Ni-metal complex were also observed. Overall, the docking analysis reveals that the various metal complexes form hydrogen bonding, carbon-hydrogen bonding, π-alkyl, π-sigma, π-anion and electrostatic type interactions.

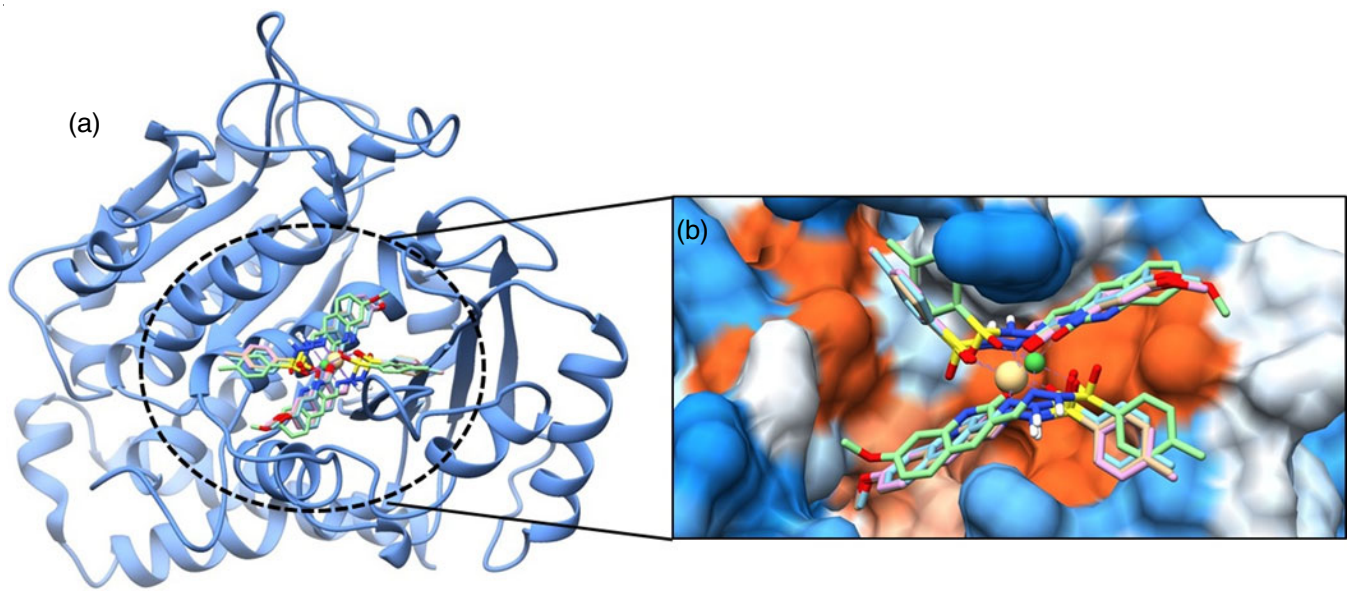

Fig. 3. Binding mode of β-tubulin with various metal complexes using molecular docking techniques. Here, (a) shows the overlapped docked conformation of Cd (cyan), Co (brown), Cu (pink) and Ni (light green) metal complexes. The N, O and H are shown in blue, red and white colours, respectively. (b) Shows electrostatic surface area of β-tubulin binding pocket with an overlapped conformation of metal complexes

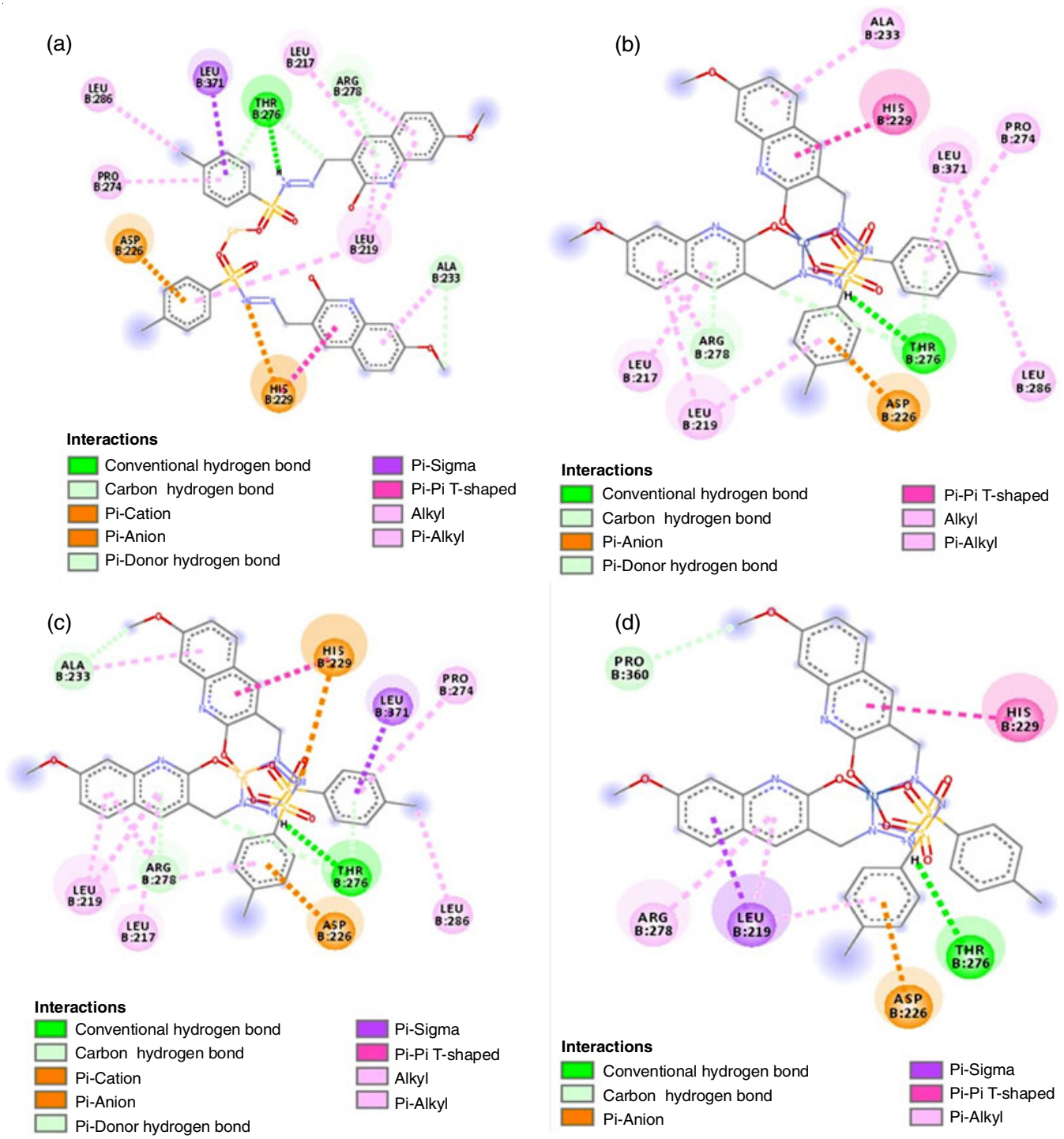

Fig. 4. 2D interactions of β-tubulin residues with metal complexes. Here, (a) shows the interaction of β-tubulin residues with the Cd-metal complex, (b) shows the interaction of β-tubulin residues with the Co-metal complex, (c) shows the interaction of β-tubulin residues with the Cu-metal complex and (d) shows the interaction of β-tubulin residues with Cd-metal complex. The 2D interaction images were generated using the Discovery Studio Visualizer

Antibacterial activity: Both Schiff base ligand and its metal(II) complexes displayed the antibacterial activity against *E. coli*, *P. aeruginosa, S. aureus* and *S. pyogenus* with MIC less than 250 µg/mL. The Schiff base ligand containing quinoline moeity displayed good antibacterial activity with the least MIC (12.5 µg/mL) against *P. aeruginosa* than standards chloramphenicol (MIC = 50 µg/mL) and ampicillin (MIC = 100 µg/mL). The Ni(II) complex displayed MIC with the highest value for *S. aureus* and *S. pyogenus* whereas Cd(II) complex for *S. aureus*. This was in accordance with the antibacterial activity displayed by standard ampicillin for *S. aureus*. Except for Cd(II) and Cu(II) complexes, formed complexes displayed good antibacterial activity than the ligand (MIC = 125 µg/mL) for *S. pyogenus*, but not like the standard chloramphenicol (MIC =

TABLE-7
ANTIMICROBIAL ACTIVITIES DATA OF QUINOLINE BASED SCHIFF BASE LIGAND AND ITS METAL COMPLEXES [MIC IN µg/mL]

Compound	Antibacterial activity				Antifungal activity		
	E. coli MTCC 443	*P. aeruginosa* MTCC 1688	*S. aureus* MTCC 96	*S. pyogenus* MTCC 442	*C. albicans* MTCC 227	*A. niger* MTCC 282	*A. clavatus* MTCC 1323
Ligand	25	12.5	50	125	250	500	500
Cu-complex	100	125	62.5	100	110	500	1000
Ni-complex	125	50	250	250	500	>1000	>1000
Co-complex	62.5	25	100	250	500	1000	1000
Cd-complex	125	125	250	100	500	>1000	>1000
Ampicillin	100	100	250	100	–	–	–
Chloramphenicol	50	50	50	50	–	–	–
Griseofulvin	–	–	–	–	500	100	100
Nystatin	–	–	–	–	100	100	100

50 µg/mL). Further, among the standards, chloramphenicol (MIC = 50 µg/mL) displayed best antibacterial activity than ampicillin (MIC = 100 and 250 µg/mL) (Table-7).

Antifungal activity: Both the Schiff base ligand and its metal(II) complexes displayed antifungal activity against *C. albicans, A. niger* and *A. clavatus* but with moderate activity than standards nystatin and griseofulvin (except from *C. albicans* with MIC 500 µg/mL). However, the most noteworthy finding is the antifungal activity of Cu complex lower activity (MIC = 110 µg/mL) compared to the experimental ligand (MIC = 250 µg/mL) (Table-7). Furthermore, Cu(II) complex displayed antifungal activity almost similar to standard griseofulvin and nystatin, thus posing its use as an antibiotic for further use.

Conclusion

A new quinoline Schiff base ligand and its metal(II) complexes were successfully synthesized and characterized by various analysis techniques. The Schiff base ligand ligand and its metal(II) complexes were screened for *in vitro* biological activity and molecular docking study. The antibacterial screening results showed that the Co(II) and Cu(II) complexes possessed good antibacterial activity and antifungal activity, respectively, compared to other metal(II) complexes. Further, *in vitro,* cytotoxicity studies showed that compared to standard paclitaxel, the Schiff-based ligand and its metal(II) complexes were more effective against the A-549 cancer cell line and less effective against the MCF-7 cancer cell line. The binding modes and interactions of metal(II) complexes with β-tubulin receptor protein are confirmed by molecular docking study. The docking studies reveal that all the metal(II) complexes show excellent binding affinity at the paclitaxel site of β-tubulin. Thus, all the synthesized compounds possessed excellent cytotoxicity properties and could be used as potential leads for cancer treatment.

ACKNOWLEDGEMENTS

The authors extend their sincere appreciation to Department of Chemistry MTES, Doshi Vakil Arts and G.C.U.B. Science & Commerce College, Goregaon, India for providing the research facilities.

CONFLICT OF INTEREST

The authors declare that there is no conflict of interests regarding the publication of this article.

REFERENCES

1. E. Raczuk, B. Dmochowska, J. Samaszko-Fiertek and J. Madaj, *Molecules*, **27**, 787 (2022); https://doi.org/10.3390/molecules27030787
2. K.T. Tadele and T.W. Tsega, *Anticancer Agents Med Chem.*, **19**, 1786 (2019); https://doi.org/10.2174/1871520619666190227171716
3. A.M.S. Hossain, J.M. Méndez-Arriaga, C. Xia, J. Xie and S. Gómez-Ruiz, *Polyhedron*, **217**, 115692 (2022); https://doi.org/10.1016/j.poly.2022.115692
4. K. Jagadesh Babu, D. Ayodhya and Shivaraj, *Results Chem.*, **6**, 10110 (2023); https://doi.org/10.1016/j.rechem.2023.101110
5. V.E. Kuz'min, A.G. Artemenko, R.N. Lozytska, A.S. Fedtchouk, V.P. Lozitsky, E.N. Muratov and A.K. Mescheriakov, *SAR QSAR Environ. Res.*, **16**, 219 (2005); https://doi.org/10.1080/10659360500037206
6. M.E. Hossain, M.N. Alam, J. Begum, M. Akbar Ali, M. Nazimuddin, F.E. Smith and R.C. Hynes, *Inorg. Chim. Acta*, **249**, 207 (1996); https://doi.org/10.1016/0020-1693(96)05098-0
7. Y. Vaghasiya, R. Nair, M. Soni, S. Baluja and S. Shanda, *J. Serb. Chem. Soc.*, **69**, 991 (2004); https://doi.org/10.2298/JSC0412991V
8. C.T. Supuran, M. Barboiu, C. Luca, E. Pop, M.E. Brewster and A. Dinculescu, *Eur. J. Med. Chem.*, **31**, 597 (1996); https://doi.org/10.1016/0223-5234(96)89555-9
9. B.K. Mallandur, G. Rangaiah and N.V. Harohally, *Synth. Commun.*, **47**, 1065 (2017); https://doi.org/10.1080/00397911.2017.1309668
10. N.G. Yernale and M.B.H. Mathada, *Bioinorg. Chem. Appl.*, **2014**, 3149 (2014); https://doi.org/10.1155/2014/314963
11. H.A. Althobiti and S.A. Zabin, *Open Chem.*, **18**, 591 (2020); https://doi.org/10.1515/chem-2020-0085
12. P.S. Salve, S.G. Alegaon and D. Sriram, *Bioorg. Med. Chem. Lett.*, **27**, 1859 (2017); https://doi.org/10.1016/j.bmcl.2017.02.031
13. A.A. Adeleke, S.J. Zamisa, M. Islam, K. Olofinsan, V.F. Salau, C. Mocktar and B. Omondi, *Molecules*, **26**, 1205 (2021); https://doi.org/10.3390/molecules26051205
14. G.T. Vidyavathi, B. Vinay Kumar, T. Aravinda and U. Hani, *Nucleosides Nucleotides Nucleic Acids*, **40**, 264 (2021); https://doi.org/10.1080/15257770.2020.1868502
15. H.R. Sonawane, B.T. Vibhute, B.D. Aghav, J.V. Deore and S.K. Patil, *Eur. J. Med. Chem.*, **258**, 115549 (2023); https://doi.org/10.1016/j.ejmech.2023.115549

16. R.M. Singh and A. Srivastava, *Indian J. Chem.*, **44**, 1868 (2005).
17. A. Rattan, Antimicrobials in Laboratory Medicine, B.I. Churchill Livingstone: New Delhi, pp. 85-108 (2000).
18. I. Wiegand, K. Hilpert and R.E.W. Hancock, *Nat. Protoc.*, **3**, 163 (2008); https://doi.org/10.1038/nprot.2007.521
19. Z. Moradi Alvand, H.R. Rajabi, A. Mirzaei and A. Masoumiasl, *New J. Chem.*, **43**, 15126 (2019); https://doi.org/10.1039/C9NJ03144H
20. P. Sharma, S. Pant, V. Dave, K. Tak, V. Sadhu and K.R. Reddy, *J. Microbiol. Methods*, **160**, 107 (2019); https://doi.org/10.1016/j.mimet.2019.03.007
21. A. Misra, S. Jain, D. Kishore, V. Dave, K.R. Reddy, V. Sadhu, J. Dwivedi and S. Sharma, *J. Microbiol. Methods*, **163**, 105648 (2019); https://doi.org/10.1016/j.mimet.2019.105648
22. A. Nagaraja, M.D. Jalageri, Y.M. Puttaiahgowda, K. Raghava Reddy and A.V. Raghu, *J. Microbiol. Methods*, **163**, 105650 (2019); https://doi.org/10.1016/j.mimet.2019.105650
23. H.R. Rajabi, R. Naghiha, M. Kheirizadeh, H. Sadatfaraji, A. Mirzaei and Z.M. Alvand, *Mater. Sci. Eng. C*, **78**, 1109 (2017); https://doi.org/10.1016/j.msec.2017.03.090
24. G.M. Morris, R. Huey, W. Lindstrom, M.F. Sanner, R.K. Belew, D.S. Goodsell and A.J. Olson, *J. Comput. Chem.*, **30**, 2785 (2009); https://doi.org/10.1002/jcc.21256
25. R.H. Wade and A.A. Hyman, *Curr. Opin. Cell Biol.*, **9**, 12 (1997); https://doi.org/10.1016/S0955-0674(97)80146-9
26. E. Nogales, *Cell. Mol. Life Sci.*, **56**, 133 (1999); https://doi.org/10.1007/s000180050012
27. R.A. Stanton, K.M. Gernert, J.H. Nettles and R. Aneja, *Med. Res. Rev.*, **31**, 443 (2011); https://doi.org/10.1002/med.20242
28. S. Gupta and B. Bhattacharyya, *Mol. Cell. Biochem.*, **253**, 41 (2003); https://doi.org/10.1023/A:1026045100219
29. B.V. Kumbhar and V.V. Bhandare, *J. Biomol. Struct. Dyn.*, (2020); https://doi.org/10.1080/07391102.2020.1745689
30. J.P. Snyder, J.H. Nettles, B. Cornett, K.H. Downing and E. Nogales, *Proc. Natl. Acad. Sci. USA*, **98**, 5312 (2001); https://doi.org/10.1073/pnas.051309398
31. J. Löwe, H. Li, K.H. Downing and E. Nogales, *J. Mol. Biol.*, **313**, 1045 (2001); https://doi.org/10.1006/jmbi.2001.5077
32. M.D. Hanwell, D.E. Curtis, D.C. Lonie, T. Vandermeersch, E. Zurek and G.R. Hutchison, *J. Cheminform.*, **4**, 17 (2012); https://doi.org/10.1186/1758-2946-4-17
33. B.V. Kumbhar, V.V. Bhandare, D. Panda and A. Kunwar, *J. Biomol. Struct. Dyn.*, **38**, 426 (2020); https://doi.org/10.1080/07391102.2019.1577174
34. W.L. DeLano, The PyMOL Molecular Graphics System, Version 1.1. Schrödinger LLC (2014); http://www.pymol.org https://doi.org/10.1038/hr.2014.17
35. W.J. Geary, *Coord. Chem. Rev.*, **7**, 81 (1971); https://doi.org/10.1016/S0010-8545(00)80009-0
36. V.V. Savant and C.C. Patel, *J. Inorg. Nucl. Chem.*, **31**, 2319 (1969); https://doi.org/10.1016/0022-1902(69)80561-0
37. M. Pervaiz, I. Ahmad, M. Yousaf, S. Kirn, A. Munawar, Z. Saeed, A. Adnan, T. Gulzar, T. Kamal, A. Ahmad and A. Rashid, *Spectrochim. Acta A Mol. Biomol. Spectrosc.*, **206**, 642 (2019); https://doi.org/10.1016/j.saa.2018.05.057
38. 36 N. Raman, A. Kulandaisamy and K. Jeyasubramanian, *Synth. React. Inorg. Met.-Org. Chem.*, **31**, 1249 (2001); https://doi.org/10.1081/SIM-100106862
39. N. Sari, S. Arslan, E. Logoglu and I. Sakiyan, *Gazi Univ. J. Sci.*, **16**, 283 (2003).
40. G. Mohamed and Z. Abd El-Wahab, *J. Therm. Anal. Calorim.*, **73**, 347 (2003); https://doi.org/10.1023/A:1025126801265
41. A.S. Salameh and H.A. Tayim, *Polyhedron*, **2**, 829 (1983); https://doi.org/10.1016/S0277-5387(00)87213-7
42. H.S. Seleem, B.A. El-Shetary and M. Shebl, *Heteroatom Chem.*, **18**, 100 (2007); https://doi.org/10.1002/hc.20239
43. M. Shebl and S.M.E. Khalil, *Monatsh. Chem.*, **145**, 146 (2015); https://doi.org/10.1007/s00706-014-1302-x
44. M. Shebl, *J. Coord. Chem.*, **62**, 3217 (2009); https://doi.org/10.1080/00958970903012785
45. M. Shebl, *J. Mol. Struct.*, **1128**, 79 (2017); https://doi.org/10.1016/j.molstruc.2016.08.056
46. P. Tyagi, S. Chandra and B.S. Saraswat, *Spectrochim. Acta A Mol. Biomol. Spectrosc.*, **134**, 200 (2015); https://doi.org/10.1016/j.saa.2014.06.112
47. D.P. Singh, R. Kumar, V. Malik and P. Tyagi, *Transition Met. Chem.*, **32**, 1051 (2007); https://doi.org/10.1007/s11243-007-0279-2
48. T.R. Rao and A. Prasad, *Synth. React. Inorg. Met.-Org. Nano-Met. Chem.*, **35**, 299 (2005); https://doi.org/10.1081/SIM-200055245
49. N.N. Greenwood and A. Earnshaw, Chemistry of the Elements. Heimemann, Oxford: UK, edn. 2 (1997).
50. T.R. Reddy and R. Srinivasan, *J. Chem. Phys.*, **43**, 1404 (1965); https://doi.org/10.1063/1.1696933
51. B.T. Thaker, P.K. Tandel, A.S. Patel, C.J. Vyas, M.S. Jesani and D.M. Patel, *Indian J. Chem.*, **44A**, 265 (2005).
52. H.F. El-Shafiy and M. Shebl, *J. Mol. Struct.*, **1156**, 403 (2018); https://doi.org/10.1016/j.molstruc.2017.11.081
53. M. Shebl, *Spectrochim. Acta A Mol. Biomol. Spectrosc.*, **73**, 313 (2009); https://doi.org/10.1016/j.saa.2009.02.030
54. H.F. El-Shafiy and M. Shebl, *J. Mol. Struct.*, **1194**, 187 (2019); https://doi.org/10.1016/j.molstruc.2019.05.063